



Numerical Scheme for the Computational Study of Two Dimensional Diffusion and Burgers' Systems with Stability and Error Estimate

Muhammad Bilal¹ · Abdul Ghafoor¹ · Manzoor Hussain² · Kamal Shah^{4,7} · Thabet Abdeljawad^{3,4,5,6}

Received: 20 November 2024 / Accepted: 20 March 2025
© The Author(s) 2025

Abstract

This paper demonstrates a numerical stratagem for the solution of two dimensional single and coupled partial differential equations, using the new version of the Haar wavelets namely: the scale-3 Haar wavelets (S3HW), combined with the finite difference formulation. The proposed method consists of two phases. The first phase deals with the numerical estimation of the temporal derivative via finite difference which converts the problem to time discrete form. The second phase describes, the approximation of the spatial derivatives along with solution, adopting S3HW. Then, the collocation technique is implemented to transform the resultant system to the set of linear algebraic equations. Solution of the linear system gives the unknown wavelet coefficients which utilized to determine the numerical solutions. Afterwards, the error, convergence, and stability analysis are conducted and deduced a new error estimate. Besides, the numerical simulations are done to verify the scheme and the obtained theoretical findings (convergence and stability). To validate, the performance of the present scheme different error measures \mathcal{L}_∞ , \mathcal{L}_2 , root mean square (RMS), and relative error (RE) are determined numerically. The scheme is also compared in terms of error with the scale-2 Haar wavelets and radial basis functions based algorithms. Overall judgement shows, that the numerical results of the developed scheme are in good agreement with the exact solution and the aforementioned methods in the literature.

Keywords Nonlinear PDEs · Scale-3 Haar wavelet · Finite difference formulation · Convergence and stability

Extended author information available on the last page of the article

1 Introduction

Most of the physical phenomena around the globe can be described by the virtue of partial differential equations (PDEs). For instance, heat conduction, standing waves, population dynamics, acoustic waves, vibration of cable structures, the underlying theory of turbulence, and shallow water waves [1–4], etc. Amongst the well-known PDEs, diffusion and Burger's equations are popular. The applications of diffusion equation can be found in various chemical, biological and physical processes [5–7]. Similarly, the flow models in fluid mechanics, gas dynamics, and non linear acoustic flow can be governed by the Burger's equation. These two equations are not only important in the mathematical modelling of various phenomena, but also used as test equations for the analysis of new numerical strategies. In this article we consider the following PDEs:

$$v_t(x, y, t) = \begin{cases} v_{xx}(x, y, t) + v_{yy}(x, y, t), & (x, y) \in \Theta, t > 0, \text{ (Diffussion equation)}, \\ \varkappa [v_{xx}(x, y, t) + v_{yy}(x, y, t)] - vv_x(x, y, t) - vv_y(x, y, t), & (x, y) \in \Theta, t > 0, \text{ (Burgers' equation)}, \end{cases} \quad (1)$$

with the following conditions:

$$v(x, y, t) = \begin{cases} f_1(x, y), & (x, y) \in \Theta, t = 0, \\ f_2(x, y, t), & (x, y) \in \partial\Theta, t \geq 0. \end{cases} \quad (2)$$

In Eq. (1), $v(x, y, t)$ describes the unknown solution, x, y , and t represent the spatial and temporal variable, respectively, Θ and $\partial\Theta$ represent the domain and its boundary, $\varkappa = \frac{1}{R}$, is the coefficient of viscosity where R represents the Reynold number, $f_1(x, y)$ and $f_2(x, y)$ are the known smooth functions.

In literature, numerous solution techniques have been proposed for the numerical study of two dimensional diffusion and Burgers' models. For example, finite difference explicit and implicit methods [8–13], finite element approaches [14–16], finite volume methods [17, 18], meshless techniques [19–22], and many more for which the readers may refer to see [23–26]. Researchers in [27] studied some new approaches for the numerical solutions of nonlinear problems.

In the recent past, wavelets inclined deep interest solving PDEs, because they poses some well-known properties like compact support, localization in space and time, and multi-resolution analysis. As a result, numerical techniques that utilize wavelet bases received considerable attention over other numerical methods. Several wavelet families have been introduced in the literature, in which the scale-2 Haar wavelet (HW) is widely implemented for the approximation of differential and integral equations (both integer and fractional order). The pioneer work addressed by Lepik [28, 29], using one and two-dimensional HW techniques to solve different kinds of PDEs. Kumar et al. [30] studied some linear and nonlinear PDEs with uniform and non-uniform HW. Oruc et al. [31–33] proposed different numerical schemes for modified Burgers', coupled Schrodinger-KdV, and regularized long wave models via scale-2 HW coupled with finite difference technique. Jiwari [34] solved Burgers' equation

by utilizing HW combined with Quasi-linearization. Later on, HW based numerical techniques have been extended in different directions for solving different problems for which the interested are referred to see the papers [35–40], and the reference therein.

Upon the successful performance of the scale-2 HW, its new version namely the scale-3 Haar wavelets (scale-3 HW) were implemented by Mittal and Pandit [41–43], in which the authors solved various kinds of differential equations and found that, the scale-3 HW converges rapidly than the scale-2 HW. In this direction, Shukla and Kumar [44] obtained the approximate solution of Burgers-Huxley equation using scale-3 HW coupled with Crank-Nicolson scheme. The same authors [45], addressed the approximate solution of fractional PDEs via Haar 3-scale wavelets. Kumar [46] implemented the scale-3 HW, to solve Klein-Gordon equations.

In the accord of literature review, the existing work on scale-3 HW is mostly related to one dimensional problems. The idea is not fully explored to high dimensional problems. Therefore, the underlying motive of this paper is to present scale-3 HW based finite difference technique for the study of two dimensional parabolic PDEs. At present, the scheme will be proposed for the diffusion equation, Burger's equation, and the system of two dimensional Burger's equations.

The remaining sections of the paper are presented in the following order. In Sect. 2, the scale-3 HW and their integrals on the interval $[A, B]$ are recalled. Section 3 is devoted to discuss the method description. Section 4 includes the error, convergence, and stability analysis of the proposed scheme. The numerical results are reported in Sect. 5 while in Sect. 6, the paper is concluded.

2 Scale-3 HW and Their Integrals

Initially, the given interval $[A, B]$ is divided into $3Q$ subintervals of equal length, and the length of each subinterval is $\delta x = \frac{B-A}{3Q}$, where $Q = 3^J$, and J represents the highest level of resolution. Next, the translation and dilation parameters are defined as $j = 0, 1, 2, 3, \dots, J$, and $k = 0, 1, 2, 3, \dots, m-1$, ($m = 3^j$), respectively. The index i represents the wavelet number which is defined for even and odd values via using $i = 3^j + 2k + 1$ and $i = 3^j + 2k + 2$. The scale-3 HW scaling function $\mathbb{H}_1(x)$, symmetric wavelet $\mathbb{H}_i^{\text{sym}}(x)$ and anti-symmetric wavelet $\mathbb{H}_i^{\text{anti-sym}}(x)$ over an arbitrary interval $[A, B]$, for $i \geq 1$ can be defined as follows [42]:

$$\mathbb{H}_1(x) = \begin{cases} 1, & x \in [A, B], \\ 0, & \text{elsewhere,} \end{cases} \quad (3)$$

$$\mathbb{H}_{i>1}^{\text{sym}}(\text{even})(x) = \frac{1}{\sqrt{2}} \begin{cases} -1, & x \in [\xi_1(i), \xi_2(i)], \\ 2, & x \in [\xi_2(i), \xi_3(i)], \\ -1, & x \in [\xi_3(i), \xi_4(i)], \end{cases} \quad (4)$$

$$\mathbb{H}_{i>1}^{\text{anti-sym}(\text{odd})}(x) = \sqrt{\frac{3}{2}} \begin{cases} 1, & x \in [\xi_1(i), \xi_2(i)), \\ 0, & x \in [\xi_2(i), \xi_3(i)), \\ -1, & x \in [\xi_3(i), \xi_4(i)), \end{cases} \tag{5}$$

where

$$\begin{aligned} \xi_1(i) &= \mathbb{A} + (\mathbb{B} - \mathbb{A})\frac{k}{m}, \quad \xi_2(i) = \mathbb{A} + (\mathbb{B} - \mathbb{A})\frac{k + 1/3}{m}, \\ \xi_3(i) &= \mathbb{A} + (\mathbb{B} - \mathbb{A})\frac{k + 2/3}{m}, \text{ and } \xi_4(i) = \mathbb{A} + (\mathbb{B} - \mathbb{A})\frac{k + 1}{m}. \end{aligned} \tag{6}$$

To solve, the given models the following repeated integrals are required:

$$P_{\zeta,i}(x) = \int_{\mathbb{A}}^x \int_{\mathbb{A}}^x \dots \int_{\mathbb{A}}^x \mathbb{H}_i(z) dz^\zeta = \frac{1}{(\zeta - 1)!} \int_{\mathbb{A}}^x (x - z)^{\zeta-1} \mathbb{H}_i(z) dz, \tag{7}$$

where $\zeta = 1, \dots, 4$, (the order of the mixed derivative), and $i = 1, 2, 3, \dots, 3\mathbb{Q}$. Following Eqs. (3)-(4), and Eq. (5), the required analytical expressions of the repeated integrals are given by [46]:

$$P_{\zeta,1}(x) = \frac{1}{\zeta!} (x - \mathbb{A})^\zeta, \tag{8}$$

$$P_{\zeta,i}^{(\text{sym})}(x) = \frac{1}{\sqrt{2}} \begin{cases} 0, & x < \xi_1(i) \\ \frac{-1}{\zeta!} \{x - \xi_1(i)\}^\zeta, & x \in [\xi_1(i), \xi_2(i)) \\ \frac{1}{\zeta!} [-\{x - \xi_1(i)\}^\zeta + 3\{x - \xi_2(i)\}^\zeta], & x \in [\xi_2(i), \xi_3(i)) \\ \frac{1}{\zeta!} [-\{x - \xi_1(i)\}^\zeta + 3\{x - \xi_2(i)\}^\zeta - 3\{x - \xi_3(i)\}^\zeta], & x \in [\xi_3(i), \xi_4(i)) \\ \frac{1}{\zeta!} [-\{x - \xi_1(i)\}^\zeta + 3\{x - \xi_2(i)\}^\zeta - 3\{x - \xi_3(i)\}^\zeta + \{x - \xi_4(i)\}^\zeta], & x > \xi_4(i), \end{cases} \tag{9}$$

$$P_{\zeta,i}^{(\text{anti-sym})}(x) = \sqrt{\frac{3}{2}} \begin{cases} 0, & x < \xi_1(i) \\ \frac{1}{\zeta!} \{x - \xi_1(i)\}^\zeta, & x \in [\xi_1(i), \xi_2(i)) \\ \frac{1}{\zeta!} [\{x - \xi_1(i)\}^\zeta - \{x - \xi_2(i)\}^\zeta], & x \in [\xi_2(i), \xi_3(i)) \\ \frac{1}{\zeta!} [\{x - \xi_1(i)\}^\zeta - \{x - \xi_2(i)\}^\zeta - \{x - \xi_3(i)\}^\zeta], & x \in [\xi_3(i), \xi_4(i)) \\ \frac{1}{\zeta!} [\{x - \xi_1(i)\}^\zeta - \{x - \xi_2(i)\}^\zeta - \{x - \xi_3(i)\}^\zeta + \{x - \xi_4(i)\}^\zeta], & x > \xi_4(i). \end{cases} \tag{10}$$

3 Description of the Method

In this section, the proposed method is outlined in sequential. In the first case, we consider the two dimensional diffusion equations, and the same strategy will be extended to two dimensional single and coupled Burgers' equation. To illustrate the procedure, let us consider the following two-dimensional model [1]:

$$v_t(x, y, t) = v_{xx}(x, y, t) + v_{yy}(x, y, t), (x, y) \in \Theta, t > 0, \quad (11)$$

subject to the following initial condition:

$$v(x, y, 0) = \eta_1(x, y), (x, y) \in \Theta, \quad (12)$$

and the associated Dirichlet boundary conditions are:

$$v(x, y, t) = \eta_2(x, y, t), (x, y) \in \partial\Theta, t > 0. \quad (13)$$

Using θ -weighted ($0 \leq \theta \leq 1$) scheme to Eq. (11), we have:

$$v^{n+1} - \delta t \theta [v_{xx} + v_{yy}]^{n+1} = v^n + \delta t (1 - \theta) [v_{xx} + v_{yy}]^n, \quad (14)$$

where $v^n = v(x, y, t^n)$, and δt is the time step size. Since, scale-3 HW are not differentiable at the end point of each subinterval therefore, the mixed highest order derivative $v_{xxyy}^{n+1}(x, y)$ is assumed via two dimensional truncated scale-3 HW series as:

$$v_{xxyy}^{n+1}(x, y) = \sum_{i=1}^{3Q} \sum_{j=1}^{3Q} a_{i,j}^{n+1} h_i(x) h_j(y), \quad (15)$$

where $a_{i,j}^{n+1}$ are the unknown coefficients of scale-3 HW, to be determined computationally. These coefficient play a pivotal role in the solution and derivative approximation. To this end, integrating Eq. (15), with respect to y from 0 to y the resultant is:

$$v_{xxy}^{n+1}(x, y) = v_{xxy}^{n+1}(x, 0) + \sum_{i=1}^{3Q} \sum_{j=1}^{3Q} a_{i,j}^{n+1} h_i(x) P_{1,j}(y). \quad (16)$$

Through integration one extra unknown term $v_{xxy}^{n+1}(x, 0)$ appeared in Eq. (16). To determine this term we integrate Eq. (16), with respect to y from 0 to 1 which gives:

$$v_{xxy}^{n+1}(x, 0) = v_{xx}^{n+1}(x, 1) - v_{xx}^{n+1}(x, 0) - \sum_{i=1}^{3Q} \sum_{j=1}^{3Q} a_{i,j}^{n+1} h_i(x) P_{2,j}(y). \quad (17)$$

Putting value from Eq. (17), in Eq. (16), and integration from 0 to y leads to:

$$v_{xx}^{n+1}(x, y) = y v_{xx}^{n+1}(x, 1) + (1 - y) v_{xx}^{n+1}(x, 0) - \sum_{i=1}^{3Q} \sum_{j=1}^{3Q} a_{i,j}^{n+1} h_i(x) [P_{2,j}(y) - y P_{2,j}(1)]. \quad (18)$$

By adopting the same procedure, one can attained the following equations:

$$v_{yy}^{n+1}(x, y) = xv_{yy}^{n+1}(1, y) + (1 - x)v_{yy}^{n+1}(0, y) - \sum_{i=1}^{3\mathbb{Q}} \sum_{j=1}^{3\mathbb{Q}} a_{i,j}^{n+1} [P_{i,2}(x) - xP_{i,2}(1)]h_j(y), \tag{19}$$

$$v_y^{n+1}(x, y) = x[v_y^{n+1}(1, y) - v^{n+1}(1, 1) + v^{n+1}(1, 0)] + (1 - x)[v_y^{n+1}(0, y) - v^{n+1}(0, 1) + v^{n+1}(0, 0)] + v^{n+1}(x, 1) - v^{n+1}(x, 0) + \sum_{i=1}^{3\mathbb{Q}} \sum_{j=1}^{3\mathbb{Q}} a_{i,j}^{n+1} [P_{i,2}(x) - xP_{i,2}(1)][P_{1,j}(y) - P_{2,j}(1)], \tag{20}$$

$$v_x^{n+1}(x, y) = y[v_x^{n+1}(x, 1) - v^{n+1}(1, 1) + v^{n+1}(0, 1)] + (1 - y)[v_x^{n+1}(x, 0) - v^{n+1}(1, 0) + v^{n+1}(0, 0)] + v^{n+1}(1, y) - v^{n+1}(0, y) + \sum_{i=1}^{3\mathbb{Q}} \sum_{j=1}^{3\mathbb{Q}} a_{i,j}^{n+1} [P_{i,1}(x) - P_{i,2}(1)][P_{2,j}(y) - yP_{2,j}(1)], \tag{21}$$

$$v^{n+1}(x, y) = y[v^{n+1}(x, 1) - v^{n+1}(0, 1)] + (1 - y)[v^{n+1}(x, 0) - v^{n+1}(0, 0)] + x[v^{n+1}(1, y) - v^{n+1}(0, y)] - xy[v^{n+1}(1, 1) + v^{n+1}(0, 1)] + x(y - 1)[v^{n+1}(1, 0) - v^{n+1}(0, 0)] + v^{n+1}(0, y) + \sum_{i=1}^{3\mathbb{Q}} \sum_{j=1}^{3\mathbb{Q}} a_{i,j}^{n+1} [P_{i,2}(x) - xP_{i,2}(1)][P_{2,j}(y) - yP_{2,j}(1)]. \tag{22}$$

Inserting Eqs. (18)- (19), and Eq. (22) in Eq. (14), and using the collocation points, $x_p = \frac{p-0.5}{3\mathbb{Q}}$; $y_q = \frac{q-0.5}{3\mathbb{Q}}$, $p, q = 1, 2, \dots, 3\mathbb{Q}$, one gets the following linear set of equations:

$$\sum_{i=1}^{3\mathbb{Q}} \sum_{j=1}^{3\mathbb{Q}} a_{i,j}^{n+1} [\mathcal{A}_{i,j}(p, q) - \theta\delta t(\mathcal{B}_{i,j}(p, q) + \mathcal{C}_{i,j}(p, q))] = \mathcal{D}^n(p, q), \tag{23}$$

where

$$\begin{aligned} \mathcal{A}_{i,j}(p, q) &= [P_{i,2}(x_p) - x_pP_{i,2}(1)][P_{2,j}(y_q) - y_qP_{2,j}(1)], \\ \mathcal{B}_{i,j}(p, q) &= h_i(x_p)[P_{2,j}(y_q) - y_qP_{2,j}(1)], \\ \mathcal{C}_{i,j}(p, q) &= [P_{i,2}(x_p) - x_pP_{i,2}(1)]h_j(y_q), \\ \mathcal{D}^n(p, q) &= v^n + \delta t(1 - \theta)[v_{xx} + v_{yy}]^n - y_q [v^{n+1}(1, 1) - v^{n+1}(0, 1)] \\ &+ (y_q - 1)v^{n+1}(1, 0) - v^{n+1}(0, 0) - x_p [v^{n+1}(1, y_q) - v^{n+1}(0, y_q)] \\ &+ x_p y_q [v^{n+1}(1, 1) - v^{n+1}(0, 1)] - x_p y_q v^{n+1}(1, 0) + x_p v^{n+1}(1, 0) \\ &- x_p(1 - y_q)v^{n+1}(0, 0) + v^{n+1}(0, y_q) + \delta t\theta [y_q v_{xx}^{n+1}(x_p, 1) \\ &+ (1 - y_q)v_{xx}^{n+1}(x_p, 0)] + \delta t\theta [x_p v^{n+1}(1, y_q) + (1 - y_q)v^{n+1}(0, y_q)]. \end{aligned} \tag{24}$$

In more compact form the system can be written as:

$$\Xi F^{n+1} = \Phi^n, \tag{25}$$

where the dimension of the coefficient matrix Ξ in Eq. (25) is $(3\mathbb{Q})^2 \times (3\mathbb{Q})^2$, while the dimension of F^{n+1} , and Φ^n is $(3\mathbb{Q})^2 \times 1$. The solution of this system gives the unknown coefficients which can be utilized in Eq. (22), to get the solution of the given equation. It is to be noted that some complex symbols have been used in the methodology part which are listed below in Table 1.

Table 1 List of mathematical symbols

Symbols	Explanation
$v_t(x, y, t)$	$\frac{\partial v(x, y, t)}{\partial t}$
$v_x(x, y, t)$	$\frac{\partial v(x, y, t)}{\partial x}$
$v_y(x, y, t)$	$\frac{\partial v(x, y, t)}{\partial y}$
$v_{xx}(x, y, t)$	$\frac{\partial^2 v(x, y, t)}{\partial x^2}$
$v_{yy}(x, y, t)$	$\frac{\partial^2 v(x, y, t)}{\partial y^2}$
$v^{n+1}(x, y)$	$v(x, y, t^{n+1})$
$v_{xxyy}^{n+1}(x, y)$	$\frac{\partial^4 v^{n+1}(x, y)}{\partial x^2 \partial y^2}$
$v_{xxy}^{n+1}(x, y)$	$\frac{\partial^3 v^{n+1}(x, y)}{\partial x^2 \partial y}$

4 Error, Convergence and Stability Analysis

This section examines the error estimate of the two dimensional scale-3 HW method (S3HWM) which leads to the convergence results as well. The stability analysis is also presented in detail. To investigate these results for the S3HWM, we demonstrate the following results.

Theorem 1 Suppose $v^{n+1}(x, y) \in L^2[\mathbb{A}, \mathbb{B}]$ and satisfies the Lipschitz condition on $[0, 1]^2$, i.e, there exists a positive constant L such that for all $(x, y_1), (x, y_2) \in [0, 1]^2$, the condition $|v^{n+1}(x, y_1) - v^{n+1}(x, y_2)| \leq L|y_1 - y_2|$ holds. Then the following error bound for $\|E_{3\mathbb{Q}}^{n+1}(x, y)\|_2$ is given by:

$$\|E_{3\mathbb{Q}}^{n+1}(x, y)\|_2 \leq \frac{L}{9\sqrt{2}} \left(\frac{1}{\mathbb{Q}}\right)^3, \tag{26}$$

where $E_{3\mathbb{Q}}^{n+1}(x, y) = v^{n+1}(x, y) - v_{3\mathbb{Q}}^{n+1}(x, y)$ in which $v_{3\mathbb{Q}}^{n+1}(x, y)$ is obtained by S3HWM and $v^{n+1}(x, y)$ is the corresponding exact value. Also S3HWM converges as $\mathbb{Q} \rightarrow \infty$ and the rate of convergence is $O\left(\frac{1}{\mathbb{Q}}\right)^3$.

Proof As $v_{3\mathbb{Q}}^{n+1}(x, y)$ is the approximation of $v^{n+1}(x, y)$ via S3HWM, then the error at the J th level of resolution is defined as:

$$\begin{aligned} E_{3\mathbb{Q}}^{n+1}(x, y) &= v^{n+1}(x, y) - v_{3\mathbb{Q}}^{n+1}(x, y) \\ &= \sum_{i=3\mathbb{Q}+1}^{\infty} \sum_{j=3\mathbb{Q}+1}^{\infty} a_{i,j}^{n+1} h_i(x) h_j(y) \\ &= \sum_{i,j=3\mathbb{Q}+1}^{\infty} a_{i,j}^{n+1} h_i(x) h_j(y). \end{aligned} \tag{27}$$

Since, $v^{n+1}(x, y) = \sum_{i=1}^{3\mathbb{Q}} \sum_{j=1}^{3\mathbb{Q}} a_{i,j}^{n+1} h_i(x) h_j(y)$ and the wavelet coefficients $a_{i,j}^{n+1}$ are deduced as follows:

$$a_{i,j}^{n+1} = \int_0^1 \int_0^1 v(x, y, t) h_i(x) h_j(y) dx dy = \langle h_i(x), \langle v(x, y, t), h_j(y) \rangle \rangle, \tag{28}$$

where $\langle \cdot, \cdot \rangle$ indicates the inner product. From the orthogonality of $h_i(x)$ on $[0, 1]$, we can write:

$$\begin{aligned} \|E_{3\mathbb{Q}}^{n+1}(x, y)\|_2^2 &= \int_0^1 \int_0^1 \left(\sum_{i,j=3\mathbb{Q}+1}^{\infty} a_{i,j}^{n+1} h_i(x) h_j(y) \right)^2 dx dy \\ &= \sum_{i,j=3\mathbb{Q}+1}^{\infty} \sum_{s,p=3\mathbb{Q}+1}^{\infty} a_{i,j}^{n+1} a_{s,p}^{n+1} \left(\int_0^1 h_i(x) h_s(x) dx \right) \\ &\quad \left(\int_0^1 h_j(y) h_p(y) dy \right) \\ &= \frac{4}{\mathbb{Q}^2} \sum_{i,j=3\mathbb{Q}+1}^{\infty} (a_{i,j}^{n+1})^2. \end{aligned} \tag{29}$$

Now, in the last expression $a_{i,j}^2$ is important to evaluate. Keeping in view, Eq. (4) and Eq. (5), one can calculate $a_{i,j}^{n+1}$ by using the following procedure:

$$\begin{aligned} \langle v^{n+1}(x, y), h_j(y) \rangle &= \int_0^1 v^{n+1}(x, y) h_j(y) dy \\ &= \frac{-1}{\sqrt{2}} \int_{\frac{k}{\mathbb{Q}}}^{\frac{k+\frac{1}{3}}{\mathbb{Q}}} v^{n+1}(x, y) dy \\ &\quad + \frac{2}{\sqrt{2}} \int_{\frac{k+\frac{1}{3}}{\mathbb{Q}}}^{\frac{k+\frac{2}{3}}{\mathbb{Q}}} v^{n+1}(x, y) dy \\ &\quad - \frac{1}{\sqrt{2}} \int_{\frac{k+\frac{2}{3}}{\mathbb{Q}}}^{\frac{k+1}{\mathbb{Q}}} v^{n+1}(x, y) dy \\ &\quad + \sqrt{\frac{3}{2}} \int_{\frac{k}{\mathbb{Q}}}^{\frac{k+\frac{1}{3}}{\mathbb{Q}}} v^{n+1}(x, y) dy \\ &\quad - \sqrt{\frac{3}{2}} \int_{\frac{k+\frac{2}{3}}{\mathbb{Q}}}^{\frac{k+1}{\mathbb{Q}}} v^{n+1}(x, y) dy \end{aligned} \tag{30}$$

Utilizing the mean value theorem for integrals which gives:

$$\begin{aligned}
\langle v^{n+1}(x, y), h_j(y) \rangle &= \frac{1}{3\mathbb{Q}} \left\{ \left(\sqrt{\frac{3}{2}} - \frac{1}{\sqrt{2}} \right) v^{n+1}(x, y_1) + \sqrt{2} v^{n+1}(x, y_2) \right. \\
&\quad \left. + \left(\frac{-1}{\sqrt{2}} - \sqrt{\frac{3}{2}} \right) v^{n+1}(x, y_3) \right\} \\
&= \frac{1}{3\mathbb{Q}} \left\{ \sqrt{\frac{3}{2}} (v^{n+1}(x, y_1) - v^{n+1}(x, y_3)) \right. \\
&\quad \left. - \frac{1}{\sqrt{2}} (v^{n+1}(x, y_1) + v^{n+1}(x, y_3)) + \sqrt{2} v^{n+1}(x, y_2) \right\} \quad (31) \\
&= \frac{1}{3\mathbb{Q}} \left\{ \sqrt{\frac{3}{2}} (v^{n+1}(x, y_1) - v^{n+1}(x, y_3)) \right. \\
&\quad \left. + \frac{1}{\sqrt{2}} (v^{n+1}(x, y_2) - v^{n+1}(x, y_1)) \right. \\
&\quad \left. + \frac{1}{\sqrt{2}} (v^{n+1}(x, y_2) - v^{n+1}(x, y_3)) \right\},
\end{aligned}$$

for some $y_1 \in (\frac{k}{\mathbb{Q}}, \frac{k+\frac{1}{3}}{\mathbb{Q}})$, $y_2 \in (\frac{k+\frac{1}{3}}{\mathbb{Q}}, \frac{k+\frac{2}{3}}{\mathbb{Q}})$, and $y_3 \in (\frac{k+\frac{2}{3}}{\mathbb{Q}}, \frac{k+1}{\mathbb{Q}})$. Now, the corresponding value of the coefficient is given as follows:

$$\begin{aligned}
a_{i,j}^{n+1} &= \langle h_i(x), \langle v^{n+1}(x, y), h_j(y) \rangle \rangle \\
&= \left\langle h_i(x), \frac{1}{3\mathbb{Q}} \left\{ \sqrt{\frac{3}{2}} (v^{n+1}(x, y_1) - v^{n+1}(x, y_3)) \right. \right. \\
&\quad \left. \left. + \frac{1}{\sqrt{2}} (v^{n+1}(x, y_2) - v^{n+1}(x, y_1)) \right. \right. \\
&\quad \left. \left. + \frac{1}{\sqrt{2}} (v^{n+1}(x, y_2) - v^{n+1}(x, y_3)) \right\} \right\rangle. \quad (32)
\end{aligned}$$

Again following the definition of inner product we can write:

$$\begin{aligned}
 a_{i,j}^{n+1} &= \frac{1}{3\mathbb{Q}} \int_0^1 \left\{ \sqrt{\frac{3}{2}}(v^{n+1}(x, y_1) - v^{n+1}(x, y_3)) + \frac{1}{\sqrt{2}}(v^{n+1}(x, y_2) \right. \\
 &\quad \left. - v^{n+1}(x, y_1)) + \frac{1}{\sqrt{2}}(v^{n+1}(x, y_2) - v^{n+1}(x, y_3)) \right\} h_i(x) dx \\
 &= \frac{1}{3\mathbb{Q}} \left\{ \int_{\frac{k}{\mathbb{Q}}}^{\frac{k+\frac{1}{3}}{\mathbb{Q}}} \sqrt{\frac{3}{2}}(v^{n+1}(x, y_1) - v^{n+1}(x, y_3)) h_i(x) dx \right. \\
 &\quad + \int_{\frac{k+\frac{1}{3}}{\mathbb{Q}}}^{\frac{k+\frac{2}{3}}{\mathbb{Q}}} \frac{1}{\sqrt{2}}(v^{n+1}(x, y_2) - v^{n+1}(x, y_1)) h_i(x) dx \\
 &\quad \left. + \int_{\frac{k+\frac{2}{3}}{\mathbb{Q}}}^{\frac{k+1}{\mathbb{Q}}} \frac{1}{\sqrt{2}}(v^{n+1}(x, y_2) - v^{n+1}(x, y_3)) h_i(x) dx \right\}. \tag{33}
 \end{aligned}$$

Using mean value theorem with little algebraic manipulation leads to:

$$\begin{aligned}
 a_{i,j}^{n+1} &= \left(\frac{1}{3\mathbb{Q}} \right)^2 \left\{ \sqrt{\frac{3}{2}} \left(\frac{-1}{\sqrt{2}} + \sqrt{\frac{3}{2}} \right) (v^{n+1}(x_1, y_1) - v^{n+1}(x_1, y_3)) \right. \\
 &\quad + (v^{n+1}(x_2, y_2) - v^{n+1}(x_2, y_1)) \\
 &\quad \left. + \frac{1}{\sqrt{2}} \left(\frac{-1}{\sqrt{2}} - \sqrt{\frac{3}{2}} \right) (v^{n+1}(x_3, y_2) - v^{n+1}(x_3, y_3)) \right\}, \tag{34}
 \end{aligned}$$

for some $x_1 \in (\frac{k}{\mathbb{Q}}, \frac{k+\frac{1}{3}}{\mathbb{Q}})$, $x_2 \in (\frac{k+\frac{1}{3}}{\mathbb{Q}}, \frac{k+\frac{2}{3}}{\mathbb{Q}})$, and $x_3 \in (\frac{k+\frac{2}{3}}{\mathbb{Q}}, \frac{k+1}{\mathbb{Q}})$. Since, the Lipschitz condition holds, therefore we get the following result:

$$\begin{aligned}
 |a_{i,j}^{n+1}| &= \left(\frac{1}{3\mathbb{Q}} \right)^2 \left| \left\{ \sqrt{\frac{3}{2}} \left(\frac{-1}{\sqrt{2}} + \sqrt{\frac{3}{2}} \right) (v^{n+1}(x_1, y_1) - v^{n+1}(x_1, y_3)) + (v^{n+1}(x_2, y_2) - v^{n+1}(x_2, y_1)) \right. \right. \\
 &\quad \left. \left. + \frac{1}{\sqrt{2}} \left(\frac{-1}{\sqrt{2}} - \sqrt{\frac{3}{2}} \right) (v^{n+1}(x_3, y_2) - v^{n+1}(x_3, y_3)) \right\} \right| \leq \left(\frac{1}{3\mathbb{Q}} \right)^2 \\
 &\quad \left\{ \left| \sqrt{\frac{3}{2}} \left(\frac{-1}{\sqrt{2}} + \sqrt{\frac{3}{2}} \right) (v^{n+1}(x_1, y_1) - v^{n+1}(x_1, y_3)) \right| \right. \\
 &\quad \left. + \left| (v^{n+1}(x_2, y_2) - v^{n+1}(x_2, y_1)) \right| + \left| \frac{1}{\sqrt{2}} \left(\frac{-1}{\sqrt{2}} - \sqrt{\frac{3}{2}} \right) (v^{n+1}(x_3, y_2) - v^{n+1}(x_3, y_3)) \right| \right\} \\
 &\leq \left(\frac{1}{3\mathbb{Q}} \right)^2 \left\{ \left(\sqrt{\frac{3}{2}} \left(\frac{-1}{\sqrt{2}} + \sqrt{\frac{3}{2}} \right) \right) L_1 |y_1 - y_3| + L_2 |y_2 - y_1| + \left(\frac{1}{\sqrt{2}} \left(\frac{-1}{\sqrt{2}} - \sqrt{\frac{3}{2}} \right) \right) L_3 |y_2 - y_3| \right\} \\
 &\leq \left(\frac{1}{3\mathbb{Q}} \right)^2 \frac{3L}{3\mathbb{Q}} = \left(\frac{1}{3\mathbb{Q}} \right)^2 \frac{L}{\mathbb{Q}}, \tag{35}
 \end{aligned}$$

where $L = \max\left\{ \sqrt{\frac{3}{2}} \left(\frac{-1}{\sqrt{2}} + \sqrt{\frac{3}{2}} \right) L_1, L_2, \frac{1}{\sqrt{2}} \left(\frac{-1}{\sqrt{2}} - \sqrt{\frac{3}{2}} \right) L_3 \right\}$, therefore:

$$(a_{i,j}^{n+1})^2 \leq \frac{L^2}{3^{2j+4}\mathbb{Q}^4} = \frac{L^2}{3^{4j+4}\mathbb{Q}^2}. \tag{36}$$

Plugging the value of $(a_{i,j}^{n+1})^2$ into Eq. (29), we get:

$$\begin{aligned}
 \|E_{3\mathbb{Q}}^{n+1}(x, y)\|_2^2 &= \frac{4}{\mathbb{Q}^2} \sum_{i,j=3\mathbb{Q}+1}^{\infty} \frac{L^2}{3^{4j+4}\mathbb{Q}^2} \\
 &= \frac{4L^2}{\mathbb{Q}^4} \sum_{i,j=3\mathbb{Q}+1}^{\infty} \frac{1}{3^{4j+4}} \\
 &= \frac{4L^2}{\mathbb{Q}^4} \sum_{j=J+1}^{\infty} \left(\sum_{i=0}^{3^j-1} \sum_{j=0}^{3^j-1} \frac{1}{3^{4j+4}} \right) \tag{37} \\
 &= \frac{4L^2}{\mathbb{Q}^4} \sum_{j=J+1}^{\infty} \frac{1}{3^{2j+4}} \\
 &= \frac{L^2}{162\mathbb{Q}^6}.
 \end{aligned}$$

Consequently,

$$\|E_{3\mathbb{Q}}^{n+1}(x, y)\|_2 \leq \frac{L}{9\sqrt{2}} \left(\frac{1}{\mathbb{Q}}\right)^3. \tag{38}$$

This shows that S3HWM will converges *i.e.*, $\lim_{\mathbb{Q} \rightarrow \infty} v_{3\mathbb{Q}}^{n+1}(x, y) = 0$. Also, the rate of convergence is of order 3 as given by:

$$\|E_{3\mathbb{Q}}^{n+1}(x, y)\|_2 = O\left(\frac{1}{\mathbb{Q}}\right)^3. \tag{39}$$

This completes the proof.

Theorem 2 The amplification matrix for the proposed method is defined by $\mathcal{W} = \mathcal{C}_1\mathcal{M}_1^{-1}\mathcal{N}_1\mathcal{C}_1^{-1}$. The S3HWM will be stable when $\rho(\mathcal{W}) \leq 1$, where $\rho(\mathcal{W})$ denotes the spectral radius.

Proof: First, we derive the amplification matrix. To this end, Eqs. (18-19), and Eq. (22) can be reformulated in matrix form as follows:

$$v_{xx}^{n+1} = \mathcal{A}_1 a^{n+1} + \mathcal{A}_2^{n+1}, \tag{40}$$

$$v_{yy}^{n+1} = \mathcal{B}_1 a^{n+1} + \mathcal{B}_2^{n+1}, \tag{41}$$

$$v^{n+1} = \mathcal{C}_1 a^{n+1} + \mathcal{C}_2^{n+1}, \tag{42}$$

where $a^{n+1} = a_{i,j}^{n+1}$, $\mathcal{A}_1, \mathcal{B}_1, \mathcal{C}_1$ and $\mathcal{A}_2, \mathcal{B}_2, \mathcal{C}_2$ describe the differentiation and solution matrices of $v_{xx}^{n+1}, v_{yy}^{n+1}$, and v^{n+1} at the collocation points and boundary terms, respectively. Now substituting Eqs. (40–42), in Eq. (14), we obtain:

$$[\mathcal{C}_1 - \delta t \theta (\mathcal{A}_1 + \mathcal{B}_1)] a^{n+1} = [\mathcal{C}_1 + \delta t (1 - \theta) (\mathcal{A}_1 + \mathcal{B}_1)] a^n + \Upsilon^{n+1}, \tag{43}$$

where

$$\Upsilon^{n+1} = \mathcal{C}_2^n - \mathcal{C}_2^{n+1} + \theta \delta t [\mathcal{A}_2^{n+1} + \mathcal{B}_2^{n+1}] + \delta t (1 - \theta) [\mathcal{A}_2^n + \mathcal{B}_2^n].$$

From Eq. (43), we can write as:

$$a^{n+1} = \mathcal{M}_1^{-1} \mathcal{N}_1 a^n + \mathcal{M}_1^{-1} \Upsilon^{n+1}, \tag{44}$$

where $\mathcal{M}_1 = [\mathcal{C}_1 - \delta t \theta (\mathcal{A}_1 + \mathcal{B}_1)]$ and $\mathcal{N}_1 = [\mathcal{C}_1 + \delta t (1 - \theta) (\mathcal{A}_1 + \mathcal{B}_1)]$. Plugging Eq. (44), in Eq. (42), we get:

$$v^{n+1} = \mathcal{C}_1 \mathcal{M}_1^{-1} \mathcal{N}_1 a^n + \mathcal{C}_1 \mathcal{M}_1^{-1} \Upsilon^{n+1} + \mathcal{C}_2^{n+1}. \tag{45}$$

Using Eq. (42), in Eq. (45), we have:

$$v^{n+1} = \mathcal{C}_1 \mathcal{M}_1^{-1} \mathcal{N}_1 \mathcal{C}_1^{-1} v^n - \mathcal{C}_1 \mathcal{M}_1^{-1} \mathcal{N}_1 \mathcal{C}_1^{-1} \mathcal{C}_2^n + \mathcal{C}_1 \mathcal{M}_1^{-1} \Upsilon^{n+1} + \mathcal{C}_2^{n+1}. \tag{46}$$

The above equation shows the time discrete scheme. If \tilde{v}^{n+1} denotes the corresponding approximate solution then:

$$\tilde{v}^{n+1} = \mathcal{C}_1 \mathcal{M}_1^{-1} \mathcal{N}_1 \mathcal{C}_1^{-1} \tilde{v}^n - \mathcal{C}_1 \mathcal{M}_1^{-1} \mathcal{N}_1 \mathcal{C}_1^{-1} \tilde{\mathcal{C}}_2^n + \mathcal{C}_1 \mathcal{M}_1^{-1} \Upsilon^{n+1} + \tilde{\mathcal{C}}_2^{n+1}. \tag{47}$$

Let $e^n = v^n - \tilde{v}^n$ be the error at the n th time level. Subtracting Eq. (46), from Eq. (47), which gives:

$$e^{n+1} = \mathcal{W} e^n, \tag{48}$$

where $\mathcal{W} = \mathcal{C}_1 \mathcal{M}_1^{-1} \mathcal{N}_1 \mathcal{C}_1^{-1}$ is the amplification matrix. According to Lax-Richtmyer criterion, the scheme will be stable if $\|\mathcal{W}\| \leq 1$ which is equivalent to $\rho(\mathcal{W}) \leq 1$.

5 Illustrative Examples

Here, the proposed numerical method is implemented to solve different problems numerically. To evaluate the performance of the method various error norms which include $\mathcal{L}_\infty, \mathcal{L}_2$, root mean square (RMS), and relative error (RE) are shown, and defined as follows:

$$\begin{aligned}
 \mathcal{L}_\infty &= \max_{1 \leq i,j \leq 3\mathbb{Q}} |v_{i,j}^{Ext} - v_{i,j}^{App}|, & \mathcal{L}_2 &= \sqrt{\sum_{i=1}^{3\mathbb{Q}} \sum_{j=1}^{3\mathbb{Q}} (v_{i,j}^{Ext} - v_{i,j}^{App})^2}, \\
 \text{RMS} &= \sqrt{\frac{\sum_{i=1}^{3\mathbb{Q}} \sum_{j=1}^{3\mathbb{Q}} (v_{i,j}^{Ext} - v_{i,j}^{App})^2}{3\mathbb{Q} \times 3\mathbb{Q}}}, \\
 \text{RE} &= \sqrt{\frac{\sum_{i=1}^{3\mathbb{Q}} \sum_{j=1}^{3\mathbb{Q}} (v_{i,j}^{Ext} - v_{i,j}^{App})^2}{\sum_{i=1}^{3\mathbb{Q}} \sum_{j=1}^{3\mathbb{Q}} (v_{i,j}^{Ext})^2}},
 \end{aligned}
 \tag{49}$$

where $v_{i,j}^{Ext}$, $v_{i,j}^{App}$, are the exact and approximate solution, respectively.

Problem 5.1 Consider the diffusion Eq. (11), with the following initial and boundary conditions:

$$\begin{aligned}
 v(x, y, 0) &= \sin(\pi x) \sin(\pi y) = \eta_1(x, y), \\
 v(0, y, t) &= v(1, y, t) = 0, \quad v(x, 0, t) = v(x, 1, t) = 0.
 \end{aligned}
 \tag{50}$$

The analytical solution of this problem is $v(x, y, t) = \exp(-2\pi^2 t) \sin(\pi x) \sin(\pi y)$. The initial condition $\eta_1(x, y) = \sin(\pi x) \sin(\pi y)$ can be obtained from the exact solution by setting $t = 0$. Numerical simulations of this problem are conducted for the spatial domain $[0, 1]^2$ and $\theta = \frac{1}{2}$. In Table 2, the obtained error norms are shown for different time $t = 0.01, 0.05, 0.1$, while varying the resolution level $J = 0, \dots, 3$. Table 2 demonstrates, the fact that accuracy changes with the resolution level, means, when J rises the accuracy increases. In the same table, a rigorous comparison in terms of \mathcal{L}_∞ error norm is presented for the effectiveness of the method. Comparison clearly indicates, the accuracy improvement over the scale-2 HW and radial basis functions techniques. Besides, solution profiles which include exact solution, numerical solution, absolute error, and the corresponding contour are displayed in Fig. 1, for the parameters $\delta t = 0.001$, $J = 2$, and $t = 0.2$, which shows the mutual agreement of the exact and numerical solutions.

Table 2 Simulation results of problem 5.1 for various values of J and t using $dt = 0.001$

J	$t = 0.01$		$t = 0.05$		$t = 0.1$	
	\mathcal{L}_∞	\mathcal{L}_2	\mathcal{L}_∞	RMS	\mathcal{L}_∞	RE
0	1.6167e-03	1.6167e-03	3.7633e-03	4.0389e-02	2.7620e-03	9.2067e-04
1	7.8039e-04	3.2931e-03	1.8428e-03	4.9444e-03	1.3772e-03	6.4572e-04
2	9.1985e-05	1.2387e-03	2.1715e-04	5.8262e-04	1.6260e-04	8.1097e-05
3	1.4905e-05	6.0358e-04	3.4767e-05	9.3281e-05	2.6001e-05	1.2999e-05
Error norms						
Methods	t	Points	\mathcal{L}_∞	RMS		
Present method	0.2	81 × 81	7.2350e-06	3.6172e-06		
HW [1]	0.2	64 × 64	1.0093e-05	5.0488e-06		
Wendlands [47]	0.2	100 × 100	1.1750e-04	6.2660e-05		
Multiquadric [47]	0.2	100 × 100	6.4300e-06	3.2610e-06		

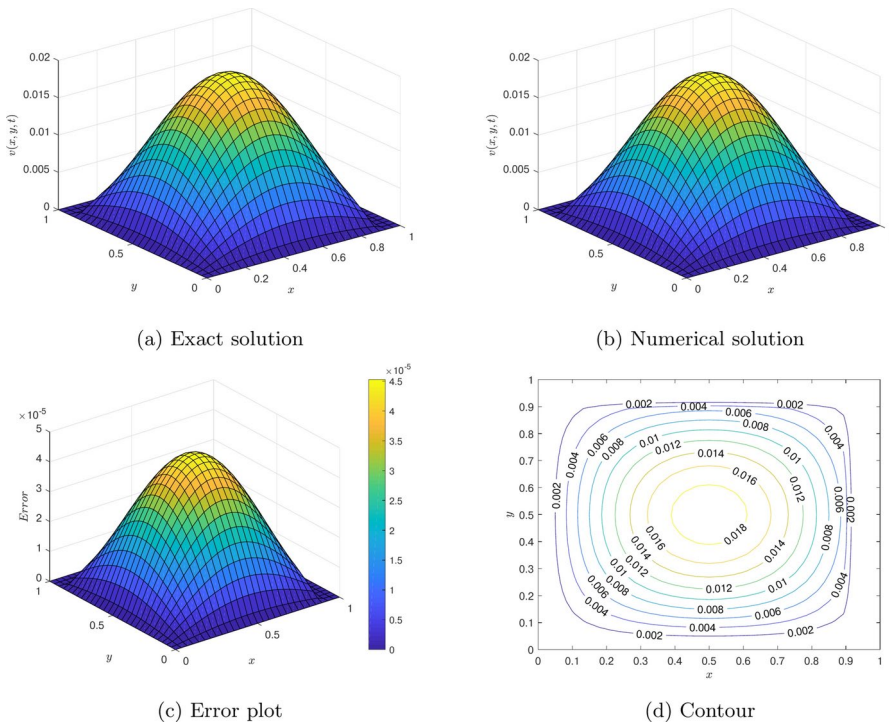


Fig. 1 Graphical solutions of problem 5.1 at $J = 2$ and $t = 0.2$

Problem 5.2 Here, we consider Eq. (11), nonlinear Burgers' equation [1, 24]:

$$v_t(x, y, t) = \varkappa[v_{xx}(x, y, t) + v_{yy}(x, y, t)] - vv_x(x, y, t) - vv_y(x, y, t). \quad (51)$$

The closed form solution of this problem is given by:

$$v(x, y, t) = \frac{1}{1 + \exp\left(\frac{x+y-t}{2\varkappa}\right)}.$$

The exact solution is used for the required initial and boundary conditions. Following the proposed methodology, the time discrete form of Eq. (51) is given as follows:

$$v^{n+1} + \delta t\theta[vv_x + vv_y]^{n+1} - \varkappa\delta t\theta[v_{xx} + v_{yy}]^{n+1} = v^n - \delta t(1 - \theta)[vv_x + vv_y]^n + \varkappa\delta t\theta[v_{xx} + v_{yy}]^n. \quad (52)$$

The nonlinear terms in Eq. (52) are linearized with the help of formulae given in [48]:

$$\begin{aligned} (vv_x)^{n+1} &= v^{n+1}v_x^n + v_x^{n+1}v^n - v^n v_x^n, \\ (vv_y)^{n+1} &= v^{n+1}v_y^n + v_y^{n+1}v^n - v^n v_y^n. \end{aligned} \quad (53)$$

Substituting Eq. (53), in Eq. (52), the following linearized form can be obtained:

$$\begin{aligned}
 &v^{n+1} + \delta t \theta [v_x^n + v_y^n] v^{n+1} + \delta t \theta [v_x^{n+1} + v_y^{n+1}] v^n - \varkappa \delta t \theta [v_{xx} + v_{yy}]^{n+1} \\
 &= v^n - \delta t (1 - 2\theta) v^n v_x^n - \delta t (1 - 2\theta) v^n v_y^n \\
 &+ \varkappa \delta t (1 - \theta) [v_{xx} + v_{yy}]^n.
 \end{aligned}
 \tag{54}$$

Now, putting the value of v^{n+1} along with its derivatives, using Eqs. (18)-(22), in Eq. (54), the desired system of linear algebraic equations for the determination of the unknown wavelet coefficients can be obtained. For the numerical experiments of this problem we chose the spatial domain $[0, 1] \times [0, 1]$, $\varkappa = 1$, $\theta = \frac{1}{2}$ and various values of δt . The \mathcal{L}_∞ and \mathcal{L}_2 error norms are shown in Table 3 for various time and $J = 2$. In the same table computed result are matched with the scale-2 HW and radial basis function method. Comparison exploits that the obtained results are in good agreement with those obtained through the scale-2 HW technique and dominate over the radial basis function method. Figure 2, shows the graphical representation of the analytical and approximate solutions, absolute error, and contour of numerical solution. Figure shows the close agreement of the numerical and exact solutions. Overall simulations of this problem show, the performance of the present method for nonlinear problems.

Problem 5.3 Finally, we consider the two-dimensional Burgers’ system given below [1]:

$$\begin{aligned}
 v_t(x, y, t) &= \varkappa [v_{xx}(x, y, t) + v_{yy}(x, y, t)] - vv_x(x, y, t) \\
 &- wv_y(x, y, t), \\
 w_t(x, y, t) &= \varkappa [w_{xx}(x, y, t) + w_{yy}(x, y, t)] - vw_x(x, y, t) \\
 &- ww_y(x, y, t),
 \end{aligned}
 \tag{55}$$

with exact solution [50]:

$$v(x, y, t) = \frac{3}{4} - \frac{1}{4} [1 + \exp((-4x + 4y - t) \frac{R}{32})]^{-1}
 \tag{56}$$

Table 3 \mathcal{L}_∞ and \mathcal{L}_2 norms at $J = 2$ for problem 5.2 at different time

Problem 5.2					
$t = 1.0, \delta t = \frac{1}{40}$		$t = 1.0, \delta t = \frac{1}{80}$		$t = 1.0, \delta t = \frac{1}{160}$	
\mathcal{L}_∞	\mathcal{L}_2	\mathcal{L}_∞	\mathcal{L}_2	\mathcal{L}_∞	\mathcal{L}_2
1.4267e-04	1.4504e-03	1.4265e-04	1.4500e-03	1.4264e-04	1.4499e-03
Error norms					
Methods	t	Points	\mathcal{L}_∞	\mathcal{L}_2	
Present method	0.5	9×9	6.1941e-05	3.1056e-04	
HW [1]	0.5	8×8	6.3677e-05	2.7799e-04	
Method in [49]	0.25	10×10	7.8844e-04	4.0331e-03	
	0.25	20×20	8.5596e-05	8.4763e-04	

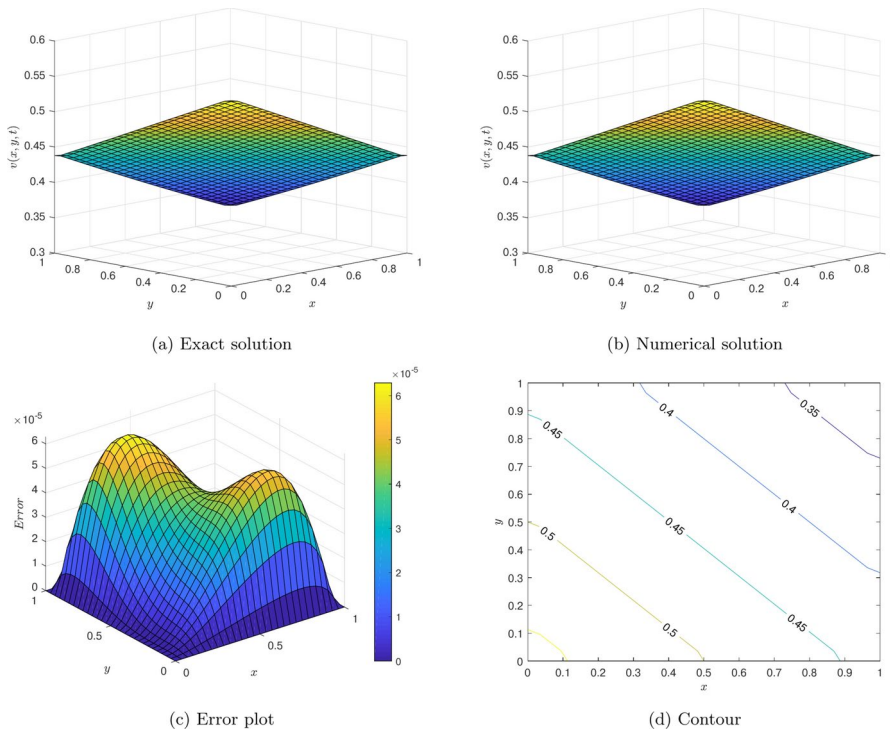


Fig. 2 Solution profiles, error and contour plot of problem 5.2 at $J = 2$ and $t = 0.5$

$$w(x, y, t) = \frac{3}{4} + \frac{1}{4} \left[1 + \exp\left(\frac{-4x + 4y - t}{32}\right) \right]^{-1}. \tag{57}$$

Using the proposed numerical method to the given system Eq. (55), gives the following system of linear equations:

$$\begin{aligned} & \sum_{i=1}^{3Q} \sum_{j=1}^{3Q} \left[b_{i,j}^{n+1} \{ \mathcal{A}_{i,j}(p, q) + \theta \delta t (\mathcal{A}_{i,j}(p, q) v_x^n + \mathcal{E}_{i,j}(p, q) v^n + \mathcal{F}_{i,j}(p, q) w^n - \varkappa (\mathcal{B}_{i,j}(p, q) \right. \\ & \left. + \mathcal{C}_{i,j}(p, q)) \} + a_{i,j}^{n+1} \delta t \theta \{ \mathcal{A}_{i,j}(p, q) v_x^n \} \right] = \mathcal{X}^n(p, q), \\ & \sum_{i=1}^{3Q} \sum_{j=1}^{3Q} [\theta \delta t b_{i,j}^{n+1} \{ \mathcal{A}_{i,j}(p, q) \} + a_{i,j}^{n+1} \{ \mathcal{A}_{i,j}(p, q) + \theta \delta t (\mathcal{A}_{i,j}(p, q) w_y^n + \mathcal{E}_{i,j}(p, q) v^n \\ & \left. + \mathcal{F}_{i,j}(p, q) w^n) - \varkappa (\mathcal{B}_{i,j}(p, q) + \mathcal{C}_{i,j}(p, q)) \}] = \mathcal{Y}^n(p, q), \end{aligned} \tag{58}$$

where $\mathcal{A}_{i,j}(p, q)$, $\mathcal{B}_{i,j}(p, q)$, $\mathcal{C}_{i,j}(p, q)$ are given in Eq. (24), and the remaining terms are described as follows:

$$\begin{aligned} \mathcal{E}_{i,j}(p, q) &= [P_{i,1}(x_p) - P_{i,2}(1)] [P_{2,j}(y_q) - y_q P_{2,j}(1)], \\ \mathcal{F}_{i,j}(p, q) &= [P_{i,2}(x_p) - x_p P_{i,2}(1)] [P_{1,j}(y_q) - P_{2,j}(1)]. \end{aligned} \tag{59}$$

Similar to $\mathcal{D}^n(p, q)$ in Eq. (23) the values of $\mathcal{X}^n(p, q)$ and $\mathcal{E}^n(p, q)$ can computed. Like the aforesaid problems, computed results are noted in the spatial domain $[0, 1] \times [0, 1]$, for both components. Table 4 contains, the numerical values of different error norms at various resolution levels and Reynold number which guarantees that error norms tends to zero as the level of resolution increases. It is also obvious from the table that accuracy is high when Reynold number is low, which reduces upon raising the Reynold number. This phenomena occurs due to the inverse proportionality of Reynold number with the coefficient of viscosity. In Table 5, comparison is given in terms of \mathcal{L}_∞ and RMS norms with earlier methods namely meshless method and scale-2 HW method. Comparison shows the clear dominance of the present scheme over the existing two numerical strategies in two dimensional coupled system. Figures 3 and 4 provide the exact versus numerical solutions together with its corresponding error and contour plots for $J = 2$, which visualize the closeness of exact and numerical solutions in both components.

6 Conclusion and Future Plan

This work showed the successful implementation of the scale-3 HW and finite difference formulation for the numerical solutions of two dimensional linear and non-linear single and coupled PDEs. Computed simulations provide the advantage of the proposed method over the existing techniques namely: scale-2 HW and meshless method particularly, radial basis function techniques. Some interesting features and precautionary measure with future directions are described as follows:

- The suggested method provides best results from the meshless technique, in terms of error norms avoiding the optimality of the shape parameter as given in [51]. Also, the scheme gives comparable results with scale-2 HW [1] method with

Table 4 Numerical results of problem 5.3 at various Reynold numbers and time

J	Points	R	δt	$t = 0.5$		$t = 1$	
				\mathcal{L}_∞	RMS	\mathcal{L}_2	RE
<i>v(x, y, t)</i>							
0	3×3	20	$\frac{1}{3}$	1.0203e-03	3.7040e-04	1.1117e-03	3.7058e-04
1	9×9	40	$\frac{1}{9}$	1.0000e-03	3.8172e-04	2.5000e-03	2.7564e-04
2	27×27	80	$\frac{1}{27}$	3.9650e-04	2.1706e-04	3.7000e-03	1.3619e-04
0	3×3	1	0.010	1.8677e-11	1.0090e-11	3.2979e-11	1.0993e-11
1	9×9	10	0.005	1.4428e-06	8.8474e-07	8.1886e-06	9.0985e-07
2	27×27	100	0.001	7.9761e-04	2.5524e-04	5.5000e-03	2.0311e-04
<i>w(x, y, t)</i>							
0	3×3	20	$\frac{1}{3}$	1.0220e-03	2.4591e-04	1.1130e-03	3.7099e-04
1	9×9	40	$\frac{1}{9}$	1.0000e-03	2.4488e-04	2.5000e-03	2.7486e-04
2	27×27	80	$\frac{1}{27}$	3.9719e-04	1.4019e-04	3.8000e-03	1.3978e-04
0	3×3	1	0.010	1.8677e-11	7.1879e-12	3.2979e-11	1.0993e-11
1	9×9	10	0.005	1.4428e-06	6.1700e-07	8.1871e-06	9.0968e-07
2	27×27	100	0.001	7.9049e-04	1.7506e-04	5.7000e-03	2.0959e-04

Table 5 Comparison results of problem 5.3 with other numerical techniques

Method	Points	R	δt	$t = 0.01$		$t = 2$	
				\mathcal{L}_∞	RMS	\mathcal{L}_∞	RMS
$v(x, y, t)$							
Present method	9×9	1	0.001	5.4578e-13	3.2877e-13	2.4201e-12	1.7405e-12
	9×9	10	0.001	5.4288e-08	3.1387e-08	2.5012e-06	1.3566e-06
	27×27	100	0.001	3.3853e-05	1.2443e-05	5.5392e-04	2.5196e-04
HW [1]	8×8	1	0.001	6.6802e-13	4.0951e-13	3.0445e-12	2.1511e-12
	8×8	10	0.001	6.8382e-08	3.8344e-08	3.2447e-06	1.6951e-06
	32×32	100	0.001	2.3469e-05	8.8124e-06	3.8865e-04	1.7851e-04
Method in [51]	10×10	1	0.0005	6.7236e-07	5.0078e-07	9.5121e-07	1.3922e-06
	20×20	100	0.001	3.3603e-06	4.5221e-07	7.6757e-05	2.5477e-05
$w(x, y, t)$							
Present method	9×9	1	0.001	5.4567e-13	2.3481e-13	2.4199e-12	1.2299e-12
	9×9	10	0.001	5.4291e-08	2.2425e-08	2.5006e-06	8.7954e-07
	27×27	100	0.001	3.3622e-05	8.9427e-06	5.5115e-04	1.3864e-04
HW [1]	8×8	1	0.001	6.6802e-13	2.9249e-13	3.0446e-12	1.5202e-12
	8×8	10	0.001	6.8385e-08	2.7396e-08	3.2438e-06	1.0992e-06
	32×32	100	0.001	2.3302e-05	6.3336e-06	3.8625e-04	9.8066e-05
Method in [51]	10×10	1	0.0005	9.4127e-07	5.0961e-07	1.3165e-06	1.3987e-06
	20×20	100	0.001	3.5901e-06	3.7169e-07	8.0991e-05	1.6227e-05

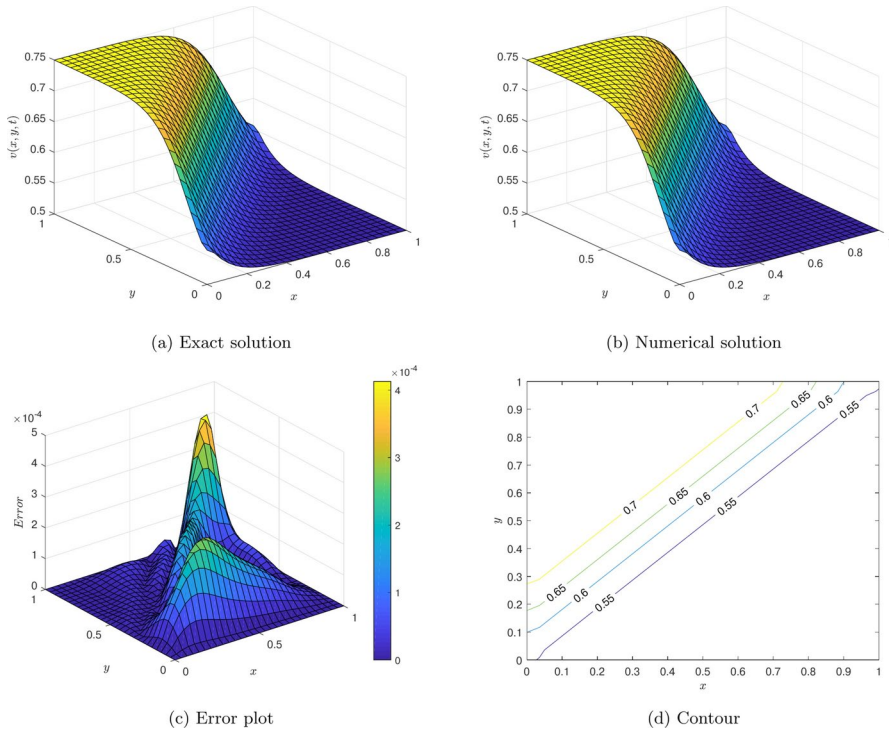


Fig. 3 Solution profiles, error and contour of problem 3, when $J = 2, t = 0.5, R = 80$ and $\delta t = 0.001$

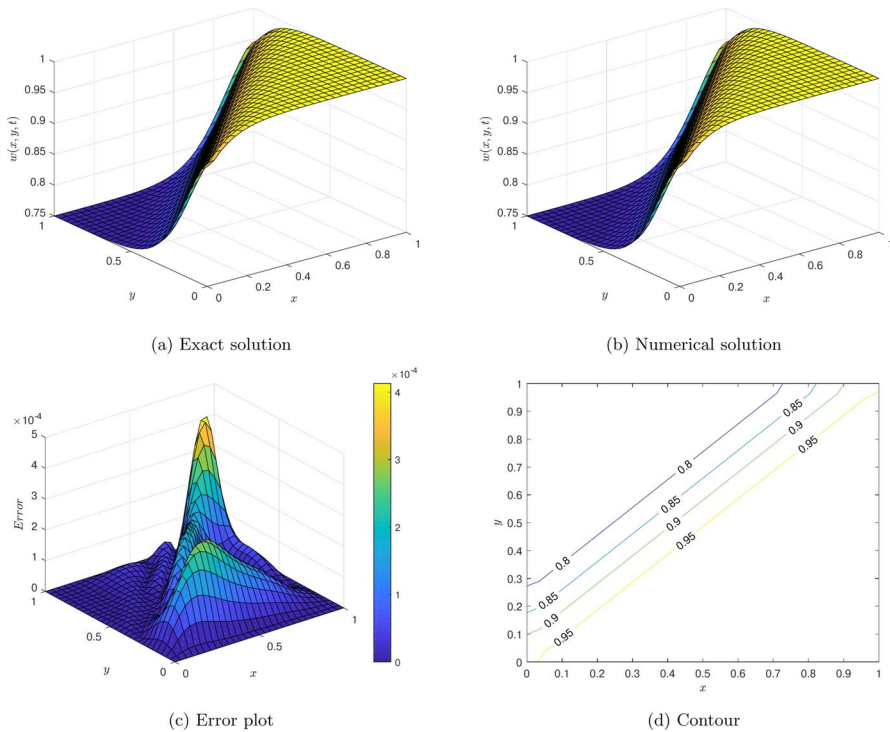


Fig. 4 Solution profiles, error plot and contour for Problem 3, when $J = 2$, $t = 0.5$, $R = 80$ and $\delta t = 0.001$

good stability and convergence properties.

- The proposed method uses the enhanced wavelet basis functions, which reduce the sparsity, to avoid the singular nature of the coefficient matrix as compared to than scale-2 HW method.
- Although, the present method works well and copes with the optimality of the shape parameter in meshless method and sparsity in the scale-2 HW method. But, it still has the issue with high resolution level which increase the computational complexity which can be tackle, up to some extent by using the proper choice of the step sizes.
- In future, the method can be extended to the higher order and multi-dimensional problems of integer and fractional problems with local and global time fractional derivative.

Acknowledgements Authors Kamal Shah and Thabet Abdeljawad are thankful to Prince Sultan University for APC and support through TAS research lab.

Author contributions Muhammad Bilal: Writing- original draft, Software, Methodology, Abdul Ghafoor: Supervision, Conceptualization, Manzoor Hussain: Reviewing original draft and editing, Visualization, Kamal Shah: Formal analysis, investigation, Thabet Abdeljawad: Funding acquisition, Resources,. All authors have read and agreed to the published version of the manuscript.

Funding Not Applicable.

Data Availability Data will be made available on request.

Declarations

Conflict of interest The authors declare no conflict of interest.

Ethics Approval Not Applicable

Open Access This article is licensed under a Creative Commons Attribution-NonCommercial-NoDerivatives 4.0 International License, which permits any non-commercial use, sharing, distribution and reproduction in any medium or format, as long as you give appropriate credit to the original author(s) and the source, provide a link to the Creative Commons licence, and indicate if you modified the licensed material. You do not have permission under this licence to share adapted material derived from this article or parts of it. The images or other third party material in this article are included in the article's Creative Commons licence, unless indicated otherwise in a credit line to the material. If material is not included in the article's Creative Commons licence and your intended use is not permitted by statutory regulation or exceeds the permitted use, you will need to obtain permission directly from the copyright holder. To view a copy of this licence, visit <http://creativecommons.org/licenses/by-nc-nd/4.0/>.

References

1. Haq, S., Ghafoor, A.: An efficient numerical algorithm for multi-dimensional time dependent partial differential equations. *Comput. Math. Appl.* **75**(8), 2723–2734 (2018)
2. Nelson, D.R.: Population dynamics and burgers' equation. *Physica A Stat. Mech. Appl.* **274**(1–2), 85–90 (1999)
3. Stanisic, M.: The mathematical theory of turbulence. Springer Science & Business Media, (2012)
4. Hereman, W.: Shallow water waves and solitary waves. In: *Sols.*, pp. 203–220. New York, NY, Springer, US (2022)
5. Pangestu, M. R. G.: "Heat equation application for modelling temperature profile in urea reactor," *Available at SSRN 4467235*
6. Ahmad, I., Ilyas, H., Hussain, S.I., Raja, M.A.Z.: Evolutionary techniques for the solution of bio-heat equation arising in human dermal region model. *Arab. J. Sci. Eng.* **49**(3), 3109–3134 (2024)
7. Caprais, M., Shviro, O., Pensec, U., Zeyen, H.: Application of the heat equation to the study of underground temperature. *Am. J. Phys.* **92**(9), 663–669 (2024)
8. Barakat, H., Clark, J.: "On the solution of the diffusion equations by numerical methods," (1966)
9. Dehghan, M.: Fully implicit finite differences methods for two-dimensional diffusion with a non-local boundary condition. *J. Comput. Appl. Math.* **106**(2), 255–269 (1999)
10. Mojumder, M.S.H., Haque, M.N., Alam, M.J.: Efficient finite difference methods for the numerical analysis of one-dimensional heat equation. *JAMP.* **11**(10), 3099–3123 (2023)
11. Bahadir, A.R.: A fully implicit finite-difference scheme for two-dimensional burgers' equations. *Appl. Math. Comput.* **137**(1), 131–137 (2003)
12. Ghafoor, A., Fiaz, M., Hussain, M., Ullah, A., Ismail, E.A., Awwad, F.A.: Dynamics of the time-fractional reaction-diffusion coupled equations in biological and chemical processes. *Sci. Rep.* **14**(1), 7549 (2024)
13. Yang, X., Ge, Y., Lan, B.: A class of compact finite difference schemes for solving the 2d and 3d burgers' equations. *Math. Comput. Simul.* **185**, 510–534 (2021)
14. Spiridonov, D., Stepanov, S., et al.: An online generalized multiscale finite element method for heat and mass transfer problem with artificial ground freezing. *J. Comput. Appl. Math.* (2023)
15. Tóth, B.: Three-field mixed hp-finite element method for the solution of the guyer-krumhansl heat conduction model. *Int. J. Heat Mass Transf.* **217**, (2023)

16. Hussein, A.J., Kashkool, H.A.: A weak galerkin finite element method for two-dimensional coupled burgers' equation by using polynomials of order $(k, k-1, k-1)$. *J. Interdiscip. Math.* **23**(4), 777–790 (2020)
17. Patel, M.R., Pandya, J.U.: Numerical study of a one and two-dimensional heat flow using finite volume. *Mater. Today: Proc.* **51**, 48–57 (2022)
18. Sheng, Y., Zhang, T.: The finite volume method for two-dimensional burgers' equation. *Pers. Ubiquitous Comput.* **22**(5), 1133–1139 (2018)
19. Kamran, Gul, U., Khan, Z. A., Haque, S., Mlaiki, N.: "A local radial basis function method for numerical approximation of multidimensional multi-term time-fractional mixed wave-diffusion and subdiffusion equation arising in fluid mechanics," *Fractal and Fract.*, vol. 8, no. 11, p. 639, (2024)
20. Reutskiy, S.: A meshless radial basis function method for 2d steady-state heat conduction problems in anisotropic and inhomogeneous media. *Eng. Anal. Bound. Elem.* **66**, 1–11 (2016)
21. Vallejo-Sánchez, J., Villegas, J.: Meshless method for the numerical solution of coupled burgers equation. *Appl. Math. Sci.* **16**(4), 205–214 (2022)
22. Aljawi, S., Aloqaily, A., Mlaiki, N. et al., "A local meshless method for the numerical solution of multi-term time-fractional generalized oldroyd-b fluid model," *Heliyon*, **10**(14), (2024)
23. Zhu, H., Shu, H., Ding, M.: Numerical solutions of two-dimensional burgers' equations by discrete adomian decomposition method. *Comput. Math. Appl.* **60**(3), 840–848 (2010)
24. Khater, A., Temsah, R., Hassan, M.: A chebyshev spectral collocation method for solving burgers'-type equations. *J. Comput. Appl. Math.* **222**(2), 333–350 (2008)
25. Alhefthi, R.K., Eltayeb, H.: The solution of two-dimensional coupled burgers' equation by g-double laplace transform. *Journal of Function Spaces* **2023**(1), 4320612 (2023)
26. Yousafzai, A., Haq, S., Ghafoor, A., Shah, K., Abdeljawad, T.: "Solution of the foam-drainage equation with cubic b-spline hybrid approach," *Phys. Scr.*, (2024)
27. Ahmad, H., Khan, T.A., Stanimirovic, P.S., Shatanawi, W., Botmart, T.: New approach on conventional solutions to nonlinear partial differential equations describing physical phenomena. *Results Phys.* **41**, (2022)
28. Lepik, Ü.: Numerical solution of evolution equations by the haar wavelet method. *Appl. Math. Comput.* **185**(1), 695–704 (2007)
29. Lepik, Ü.: Solving pdes with the aid of two-dimensional haar wavelets. *Comput. Math. Appl.* **61**(7), 1873–1879 (2011)
30. Kumar, N., Verma, A.K., Agarwal, R.P.: Two-dimensional uniform and non-uniform haar wavelet collocation approach for a class of nonlinear pdes. *Computation* **11**(10), 189 (2023)
31. Oruç, Ö., Bulut, F., Esen, A.: A haar wavelet-finite difference hybrid method for the numerical solution of the modified burgers' equation. *J. Math. Chem.* **53**, 1592–1607 (2015)
32. Oruç, Ö., Esen, A., Bulut, F.: A haar wavelet collocation method for coupled nonlinear schrödinger-kdv equations. *Int. J. Mod. Phys. C* **27**(09), 1650103 (2016)
33. Oruç, Ö., Bulut, F., Esen, A.: Numerical solutions of regularized long wave equation by haar wavelet method. *Mediterr. J. Math.* **13**(5), 3235–3253 (2016)
34. Jiwari, R.: A haar wavelet quasilinearization approach for numerical simulation of burgers' equation. *Comput. Phys. Commun.* **183**(11), 2413–2423 (2012)
35. Majak, J., Pohlak, M., Eerme, M., Lepikult, T.: Weak formulation based haar wavelet method for solving differential equations. *Appl. Math. Comput.* **211**(2), 488–494 (2009)
36. Khan, A., Ghafoor, A., Khan, E., Shah, K., Abdeljawad, T.: Solving scalar reaction diffusion equations with cubic non-linearity having time-dependent coefficients by the wavelet method of lines. *NHM* **19**(2), 634–654 (2024)
37. Haq, S., Ghafoor, A., Hussain, M.: Numerical solutions of variable order time fractional $(1+ 1)$ - and $(1+ 2)$ -dimensional advection dispersion and diffusion models. *Appl. Math. Comput.* **360**, 107–121 (2019)
38. Mrázek, P., Weickert, J.: From two-dimensional nonlinear diffusion to coupled haar wavelet shrinkage. *J. Vis. Commun. Image Represent.* **18**(2), 162–175 (2007)
39. Chen, C.F., Hsiao, C.-H.: Haar wavelet method for solving lumped and distributed-parameter systems. *IEE Proc., Part D.* **144**(1), 87–94 (1997)
40. Ghafoor, A., Fiaz, M., Shah, K., Abdeljawad, T.: "Analysis of nonlinear burgers equation with time fractional atangana-baleanu-caputo derivative," *Heliyon*, vol. 10, no. 13, (2024)
41. Mittal, R., Pandit, S.: Quasilinearized scale-3 haar wavelets-based algorithm for numerical simulation of fractional dynamical systems. *Eng. Comput.* **35**(5), 1907–1931 (2018)

42. Mittal, R., Pandit, S.: New scale-3 haar wavelets algorithm for numerical simulation of second order ordinary differential equations. *Proceedings of the National Academy of Sciences, India Section A: Physical Sciences* **89**, 799–808 (2019)
43. Mittal, R., Pandit, S.: Sensitivity analysis of shock wave burgers' equation via a novel algorithm based on scale-3 haar wavelets. *Int. J. Comput. Math.* **95**(3), 601–625 (2018)
44. Shukla, S., Kumar, M.: Error analysis and numerical solution of burgers-huxley equation using 3-scale haar wavelets. *Eng. Comput.* **38**(1), 3–11 (2022)
45. Shukla, S., Kumar, M.: Numerical simulation of time and space fractional partial differential equation via 3-scale haar wavelet. *Int. J. Appl. Comput. Math.* **8**(4), 160 (2022)
46. Kumar, R.: "Investigation for the numerical solution of klein-gordon equations using scale 3 haar wavelets," in *Journal of Physics: Conference Series*, vol. 2267, p. 012152, IOP Publishing, 2022
47. Uddin, M.: On the selection of a good value of shape parameter in solving time-dependent partial differential equations using rbf approximation method. *Appl. Math. Model.* **38**(1), 135–144 (2014)
48. Rubin, S. G., Graves Jr, R. A.: "A cubic spline approximation for problems in fluid mechanics," *Tech. Rep.*, (1975)
49. Hussain, I., Mukhtar, S., Ali, A.: A numerical meshless technique for the solution of the two dimensional burger's equation using collocation method. *World Appl. Sci. J* **23**(12), 29–40 (2013)
50. Fletcher, C.A.: Generating exact solutions of the two-dimensional burgers' equations. *Int. J. Numer. Methods Fluids* **3**, 213–216 (1983)
51. Ali, A., ul Islam, S., Haq, S.: "A computational meshfree technique for the numerical solution of the two-dimensional coupled burgers' equations," *International Journal for Computational Methods in Engineering Science and Mechanics*, vol. 10, no. 5, pp. 406–422, 2009

Authors and Affiliations

Muhammad Bilal¹ · Abdul Ghafoor¹ · Manzoor Hussain² · Kamal Shah^{4,7} · Thabet Abdeljawad^{3,4,5,6}

✉ Abdul Ghafoor
abdulghafoor@kust.edu.pk

✉ Thabet Abdeljawad
tabdeljawad@psu.edu.sa

Muhammad Bilal
muhammadbilal204020@gmail.com

Manzoor Hussain
manzoor366@gmail.com

Kamal Shah
kshah@psu.edu.sa; kamal@uom.edu.pk

¹ Institute of Numerical Sciences, Kohat University of Science and Technology, Kohat, KP 26000, Pakistan

² Computational & Applied Mathematics Lab, Department of Mathematics, Faculty of Science & Technology, Women University of Azad Jammu & Kashmir, Bagh 12500, Pakistan

³ Department of Mathematics, Saveetha School of Engineering, Saveetha Institute of Medical and Technical Sciences, Saveetha University, Chennai 602105, India

⁴ Department of Mathematics and Sciences, Prince Sultan University, 11586 Riyadh, Saudi Arabia

⁵ Department of Medical Research, China Medical University, Taichung 40402, Taiwan

- ⁶ Department of Mathematics and Applied Mathematics, School of Science and Technology, Sefako Makgatho Health Sciences University, Ga-Rankuwa, South Africa
- ⁷ Department of Mathematics, University of Malakand, Chakdara, Dir (L), KP, Pakistan